Electronic Supplementary Material (ESI) for Journal of Materials Chemistry B.
This journal is © The Royal Society of Chemistry 2022

Supporting Information

Multifunctional AuPd-Cluster Nanotheranostics with Cascaded Self-Regulating Redox Tumor-Microenvironment for Dual-Photodynamic Synergized Enzyme Catalytic Therapy

Shilei Ren,[‡,a] Rong Dai,[‡,b] Ziliang Zheng,[‡,b] Xuejiao Chen,[b] Shutong Wu,[b] Ruiping Zhang,[*,b] and Zhiguo Gui[*,a]

[a] *Shanxi Provincial Key Laboratory for Biomedical Imaging and Big Data, College of Information and Communication Engineering, North University of China, Taiyuan 030051, China.*

[b] *Department of Radiology, First hospital of Shanxi Medical University, Taiyuan, 030001, China.*

[‡] These authors contributed equally to this work and should be considered cofirst authors.

Correspondence: E-mail: zrp_7142@sxmu.edu.cn (R. Zhang).

Correspondence: E-mail: gzgtg@163.com (Z. Gui).

Keywords: Cluster Nanotheranostics, All-in-One Nanoplatforms, NIR-II FL/PA Imaging, Photodynamic Therapy, Alloy

Experimental Section

1. Chemicals and Materials:

Gold(III) chloride trihydrate ($HAuCl_4$), Potassium hexachloropalladate (IV) (K_2PdCl_6) were purchased from Sigma-Aldrich. Bovine serum albumin (BSA) and glutathione (GSH) were bought from Aladdin Biochemical Technology Co., Ltd. 3,3′5,5′-tetramethylbenzidine (TMB, 99%), 1,3-diphenylisobenzofuran (DPBF), 5,5-dimethyl-1-pyrroline N-oxide (DMPO) and 2′,7′-dichlorodihydrofluorescein diacetate (DCFH-DA) were purchased from Sigma-Aldrich. MitoSOX Red mitochondrial superoxide indicator was acquired from Shanghai Haling Biological Technology Co., Ltd. Methylene blue (MB, 82%) were purchased from Sinopharm Chemical Reagent Co., Ltd. 3′-(p-hydroxyphenyl) fluorescein (HPF) and singlet oxygen sensor green (SOSG) were acquired from Shanghai Maokang Biotechnology Co., Ltd. (Shanghai, China). AO/EB Double Staining Kit was purchased from Beijing Solarbio Science & Technology Co., Ltd. The murine breast cancer 4T1 cell line (4T1 cells) and human umbilical veinendothelial cells (HUVEC) were supplied by Jennio Biotech Co., Ltd. Dulbecco's modified Eagle's medium (DMEM) and fetal bovine serum (FBS) were purchased from Gibco BRL Co., Ltd. All chemicals were of analytical grade and used directly without further purifications. Ultrapure water was obtained from a Milli-Q water purification system throughout the whole experiment.

2. Characterization:

The morphologies and elemental maps of AuPd-BSA cluster nanotheranostics were characterized by transmission electron microscopy (TEM) with a Tecnai G2 F20 S-twin

transmission electron microscope (FEI). The UV-vis-NIR absorption spectrum was recorded by a Cary 6000i UV-vis-NIR spectrophotometer. A Nano-Zetasizer (Malvern Instruments Ltd.) was applied to analyze the size distribution and zeta potential of AuPd-BSA CNs. X-ray photoelectron spectroscopy (XPS) was performed with a Thermo Scientific K-Alpha spectrometer using Al Kα radiation (1486.6 eV, 150 W). Fourier-transform infrared (FT-IR) spectroscopy was obtained on a Vertex Perkin-Elmer 580BIR Spectrophotometer (Bruker) using the KBr pellet technique. The blood routine test was conducted on the automatic hematology analyzer (DF52Vet, Dymind Biotech, China). Thermogravimetric analysis (TG-DTA, Rigaku, TG8101D) was performed from room temperature to 850 °C with a heating rate of 10 °C min^{-1} in an air atmosphere. The NIR-II fluorescence emission spectra were performed on a fluorescence spectrometer (Suzhou NIR-Optics Co., Ltd., China) with an 808 nm laser. The content of Au and Pd elements in the samples or organs was monitored by inductively coupled plasma atomic emission spectroscopy (ICP-AES, Jena, Plasma Quant®MS). Fluorescence microscopy images were performed by a fluorescence microscope (Olympus IX73). In vivo NIR-II fluorescence imaging and fluorescence signal of cluster nanotheranostics were collected with NIR-OPTICS Series III 900/1700 small animal imaging system (Suzhou NIR-Optics Technology Co., Ltd., China) equipped with a 1000 nm long wave pass filter (1000 LP) and 808 nm laser source. The PA properties were investigated by using a real-time multispectral optoacoustic tomographic (MSOT) imaging system. The H&E staining of tumor slices were observed by an Eclipse CI Optical Microscope (Nikon, Japan).

3. Synthesis of AuPd-BSA cluster nanotheranostics:

The cluster nanotheranostics were synthesized using BSA as the stabilizer and by a facile one-pot chemical reduction. $HAuCl_4$ (4 mL, 50 mg mL^{-1}), K_2PdCl_6 (0.6 mL, 5 mg mL^{-1}) and glutathione (4.5 mL, 50 mM) were added to ultrapure water under vigorous stirring for 15 min. Secondly, the BSA was added to the above solution with vigorous stirring another 15 min before adding NaOH to adjust the pH to strongly alkaline. Thirdly, the reaction mixture was stirred under a gentle CO flow for 15 min and then further stirred at room temperature for 24 h. Finally, the resulting products were collected after concentrated by using the rotary evaporator and washed with methanol several times.

4. To confirm the content of Au and Pd in AuPd-BSA CNs by ICP experiment:

The AuPd-BSA CNs were analyzed via ICP experiment to examine the constitution, and to confirm the content of Au and Pd. First, the AuPd-BSA CNs (800 μg mL^{-1}) were dissolved in ultrapure water. Then, the content of Au and Pd were measured by Agilent 5110 after microwave digestion.

5. The detection of ROS in vitro:

5.1 The detection of Hydroxyl Radicals (•OH):

TMB kits were used to determine the generated of •OH by AuPd-BSA CNs according to the manufacturer's instruction. TMB (10 μL, 10 mM) was added into AuPd-BSA CNs solution in the presence of various concentrations of H_2O_2 (0-80 mM) in PBS buffer (pH=6.5). The concentration of the •OH was determined by measuring the absorbance at 652 nm. All experiments were repeated at least three times with the same

outcome.

The steady-state kinetic analysis was performed at 42°C in PBS solution (pH 6.5) with AuPd-BSA CNs (800 μg mL^{-1}) as a catalyst in the presence of TMB (0.5 mM) and different concentrations of H_2O_2 (0, 5, 10, 20, 40, 60, and 80×10^{-3} M) as substrates. The absorbance of oxTMB was recorded in a time-scan mode at 652 nm through UV-vis spectrophotometer. For each H_2O_2 concentration, the initial reaction rates (V_0) were calculated from the absorbance changes by Beer-Lambert Law, and The rates were plotted against H_2O_2 content and then fitted with the Michaelis-Menten curves. Furthermore, a linear double-reciprocal plot was used for determining the K_m and V_{max}.

5.2 The detection of superoxide anion ($O_2^{\bullet-}$):

OFR was used to detect the generation of $O_2^{\bullet-}$ by AuPd-BSA CNs under the 660 nm NIR laser. First, the AuPd-BSA CNs were dissolved in ultrapure water at a concentration of 800 μg mL^{-1} OFR. Then, the solution was irradiated with a 660 nm NIR laser for different time and the concentration of the generated $O_2^{\bullet-}$ was calculated from the absorbance at 530 nm.

5.3 The detection of singlet oxygen ($^1O_2$):

The 1,3-diphenylisobenzofuran (DPBF) was used to the $^1O_2$ detection produced in the process of type-II of PDT. 4 μL of DPBF (5 mM) were added to AuPd-BSA CNs aqueous solution (2 mL, 800 μg mL^{-1}) and then the solution was irradiated with the 660 nm NIR laser under hypoxic atmospheres. The concentration of $^1O_2$ was calculated by measuring the absorbance at 410 nm.

6. The detection of •OH and $^1O_2$ by Electron spin resonance (ESR):

Electron spin resonance (ESR) technology was applied to detect the existence of singlet oxygen and free radicals. The ESR measurement were carried out as follows: AuPd-BSA CNs (800 μg mL^{-1}) were dissolved in ultrapure water, then TEMP or DMPO was added with ultrasonic dispersion, after which, irradiated them with 660 nm laser.

7. GSH consumption in vitro:

To confirm the time-dependent GSH consumption, AuPd-BSA CNs (800 μg mL^{-1}) was co-incubated with GSH (20 μL, 1.0 mM) and 5,5'-dithiobis-(2-nitrobenzoic acid) (DTNB) (5 μL, 10 mg mL^{-1}) in PBS solution (pH 6.5) at varied time (0, 0.5, 1, 2, 4, 6 and 12 h). Afterwards, the mixture solution at different reaction times was centrifugated and the supernatant was required for the GSH depletion measurement by UV-vis absorbance at 412 nm.

8. GSSG content and residual GSH content in vitro:

Similar to the GSH consumption in vitro, AuPd-BSA CNs (800 μg mL^{-1}) was mixed with GSH (20 μL, 1.0 mM) in 2 mL of PBS solution (pH 6.5) at 42 ℃. At desired time points (0, 5, 10, 15, 30 and 60 min), the residual GSH content was detected with 5,5'-dithiobis-(2-nitrobenzoic acid) (DTNB) (5 μL, 10 mg/mL). Simultaneously, GSSG content was assessed using GSH/GSSG assay kit following the manufacture's protocol (Sinobestbio, YX-C-A201). All reactions were monitored by measuring the absorbance at 412 nm after different reaction times.

9. Cell culture and AuPd-BSA CNs uptake measurement:

The 4T1 cells and HUVEC were cultured in Roswell Park Memorial Institute 1640 medium (RPMI-1640) containing 10% (v/v) fetal bovine serum (FBS) and 1%

antibiotics (penicillin-streptomycin) under 5% CO_2 atmosphere at 37 ℃. To monitor the cellular uptake of AuPd-BSA CNs, 4T1 cells were treated with AuPd-BSA CNs (500 μg mL^{-1}) for different times (0, 0.5, 1 or 2 h) at 37 °C, and then the images were observed with NIR-II fluorescence microscope (1000 nm LP, 100 ms, 808 nm excitation, 300 mW cm^{-2}).

10. Cytotoxicity assessment and apoptosis assay of AuPd-BSA CNs:

Cell viability of AuPd-BSA CNs against HUVEC was measured by a standard Cell Counting Kit (CCK8, BOSTER, China) assay. The HUVEC were seeded in 96-well microplates at a density of 1.0×10^4 cells per well for 2 h and the fresh medium dissolving various concentrations of AuPd-BSA CNs were added into the corresponding wells. After further incubation for 24 h, the FBS-free medium containing 10% CCK8 was replaced to each well for an additional 1.2 h under the same condition. Finally, the cells viability was calculated by measuring the absorbance at 450 nm using a microplate reader (BioTek Epoch 2).

To test apoptosis of AuPd-BSA CNs, 4T1 cells were seeded in 96-well plates with a density of 1.0×10^4/well at 37 °C for 12 h, and then co-incubated with the AuPd-BSA CNs at gradient concentrations (0-1000 μg mL^{-1}). The plate was exposed to a 660 nm laser. After an additional 12 h of incubation with glucose, the medium was replaced by the FBS-free medium containing 10 % CCK8 and incubated for 1.5 h under the same condition. Finally, the cell apoptosis was calculated from the absorbance at 450 nm.

11. In vitro intracellular ROS detection:

11.1 Intracellular total ROS detection:

The total ROS generation was monitored by CLSM using 2,7-dichlorofluorescein diacetate (DCFH-DA) fluorescent probe. Typically, 4T1 cells were seeded at a density of 1×10^5/well in 6-well culture plates, incubating for 24 h at 37 °C. The cells were divided into five groups: (1) PBS, (2) AuPd-BSA CNs, (3) AuPd-BSA CNs+glucose, (4) AuPd-BSA CNs+glucose+Laser+Normoxic, (5) AuPd-BSA CNs+glucose+Laser +Hypoxic. Briefly, 4T1 cells were incubated with 500 μg mL^{-1} AuPd-BSA CNs for 12 h. Subsequently, the groups (4) and (5) were illuminated by laser (660 nm) for 15 min, then the cells were stained by DCFH-DA (10 μM) and incubated for 25 min, followed by washing with PBS for twice. And the fluorescence intensities of DCFH-DA were measured by confocal laser scanning microscope.

11.2 Intracellular •OH detection:

The 4T1 cells were incubated with 500 μg $mL^{-1}$of AuPd-BSA CNs for 6 h followed by incubation with 10 μM HPF for another 30 min. After being washed by PBS buffer for three times, cells were irradiated with 660 nm NIR laser at a power density of 0.5 mW for 15 min. Then, the green fluorescence was immediately observed using CLSM with the excitation wavelength of 488 nm, and emission collection wavelength from 510 nm to 550 nm.

11.3 Intracellular $O_2^{\bullet-}$ detection:

The 4T1 cells were incubated with 500 μg mL^{-1} of AuPd-BSA CNs for 6 h followed by incubation with 5 μM MitoSOX™ for another 30 min. After being washed by PBS buffer for three times, cells were irradiated with 660 nm NIR laser at a power density of 0.5 mW for 15 min. Then, the green fluorescence was immediately observed using

CLSM with the excitation wavelength of 525 nm, and emission collection wavelength from 510 nm to 580 nm.

11.4 Intracellular $^1O_2$ detection:

The 4T1 cells were incubated with 500 μg mL^{-1} of AuPd-BSA CNs for 6 h followed by incubation with 2.0 μM SOSG for another 30 min. After being washed by PBS buffer for three times, cells were irradiated with 660 nm NIR laser at a power density of 0.5mW for 15 min. Then, the green fluorescence was immediately observed using CLSM with the excitation wavelength of 488 nm, and emission collection wavelength from 500 nm to 550 nm.

12. Live/Dead cell staining assay:

The 4T1 cells were seeded into 96-well plates and divided into five groups with different treatments. The cells were stained with AO/EB mixed dyes for 30 min. After rinsed with PBS, the cells were observed on an inverted fluorescence microscope (Olympus IX73).

13. Flow cytometer analysis of annexin V-FITC/PI-stained cells:

To test apoptosis and comfirm the PDT induced by AuPd-BSA CNs after different treatments in vitro, 4T1 were incubated with AuPd-BSA CNs (500 μg mL^{-1}) for 16 h, then rinsed with cold PBS and immediately dyed with Annexin V-FITC/PI kit (Annexin V-FITC Apoptosis Detection Kit, Solarbio), followed by detection using flow cytometry (Navios, Beckman).

14. Animal model:

All animal experiments were conducted according to the protocols approved by the

Institutional Animal Care and Use Committee of the Animal Experiment Center of Shanxi Medical University (No.2016LL141, Taiyuan, China). Male Balb/c mice (6-8 weeks) were purchased from Weitong Lihua Experimental Animal Technology Co. Ltd (Beijing). Tumor-bearing mice were established by subcutaneous injecting 4T1 cells (1×10^6) in the right thigh of mice. Tumor-bearing mice were used in experiments when the tumor volume approached 80-100 mm^3.

15. In vivo dual-modal imaging:

The 4T1 tumor-bearing mice were intravenously injected with AuPd-BSA CNs (20.0 mg kg^{-1}). The NIR-II FL and PA imaging were performed using II900/1700 *in vivo* imaging system (Suzhou NIR-Optics Co., Ltd., China) and multispectral optoacoustic tomographic (MSOT) imaging system, respectively, at different time points.

16. Biodistribution analysis:

Then, a biodistribution experiment was performed. 4T1 tumor-bearing mice were treated with intravenous injection of AuPd-BSA CNs. The mice were dissected separately at 8, 12, 24 post-injection, and the major organs (heart, spleen, liver, kidney, and lung) as well as the tumors were measured. Then, the tissues were digested with H_2O_2 and HNO_3 (volume ratio=2:1) at 80 °C, and diluted about 100 times with deionized water. The content of Au and Pd elements in the solutions was determined by ICP-AES.

17. In vivo anti-tumor test:

To evaluate the anti-tumor effects, 4T1 tumor-bearing BALB/c mice with tumor volume reached 80~100 mm^3 were randomly divided into five groups (n=4 mice per

group): (1) PBS + Laser, (2) Au-BSA CNs, (3) AuPd-BSA CNs, (4) Au-BSA CNs + Laser, (5) AuPd-BSA CNs + Laser. The tumor region was irradiated with NIR laser (1.0 W cm^{-2}, 15 min) after 8 h i.v. injection (10 mg kg^{-1}) of AuPd-BSA CNs. Tumor volume was calculated as $(a \times b)^2/2$, where a and b are the tumor length and tumor width, respectively. Relative body weight is defined as W/W_0, and W_0 is the initial body weight of mice. The major organs (heart, liver, spleen, lung and kidney) as well as tumors were collected for hematoxylin and eosin (H&E) staining.

18. In vivo biocompatibility assay:

6-8 weeks old BALB/c mice were randomly divided into 5 groups (n = 4), which intravenously injected with PBS, Au-BSA and AuPd-BSA, respectively. Comprehensive blood biochemical analysis were performed on mice at 15 days after intravenous administration.

19. Statistical analysis:

All experimental data were indicated as means (standard deviation), and a statistical significance was considered significance as a value of *P < 0.05, **P < 0.01, ***P < 0.001, n.s. = not significant, respectively.

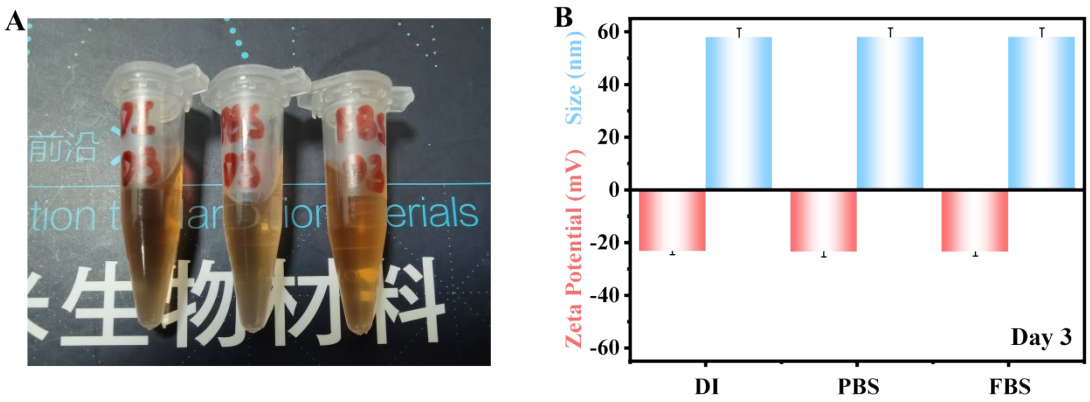

Figure S1. A) The digital photographs of AuPd-BSA CNs in DI, PBS and FBS. B) The DLS and zeta potentials of AuPd-BSA CNs dispersed in different solutions including in DI, PBS and FBS at 37 °C within 3 days.

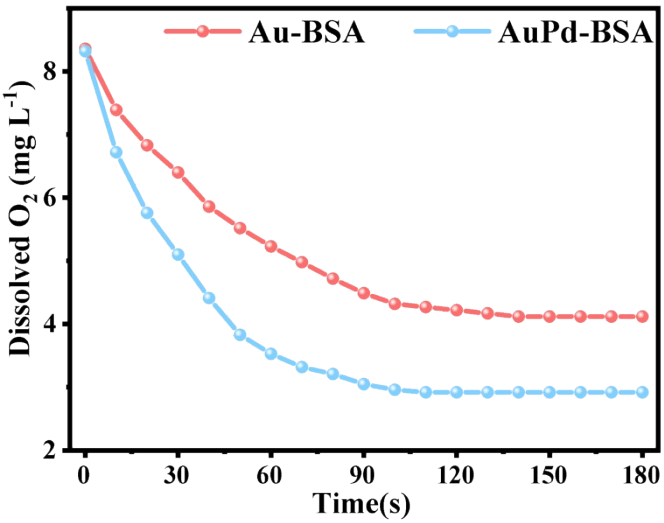

Figure S2. The detection of the dissolved oxygen after treated with AuPd-BSA and Au-BSA (800 μg mL^{-1}) in the presence of glucose, respectively.

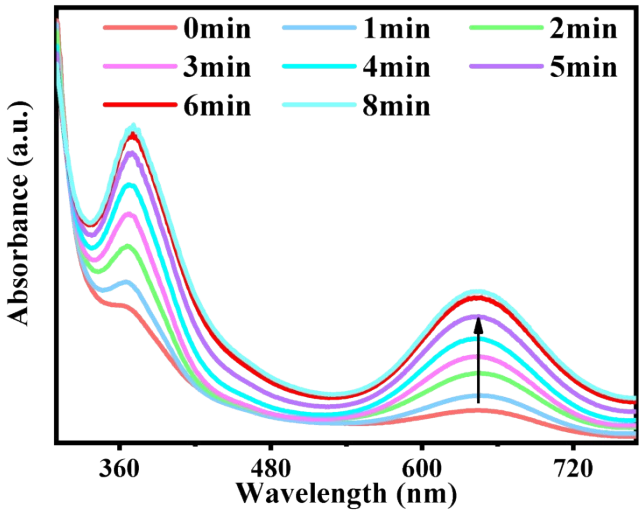

Figure S3. Time-dependent absorption changes of oxTMB in the presence of AuPd-BSA and H_2O_2.

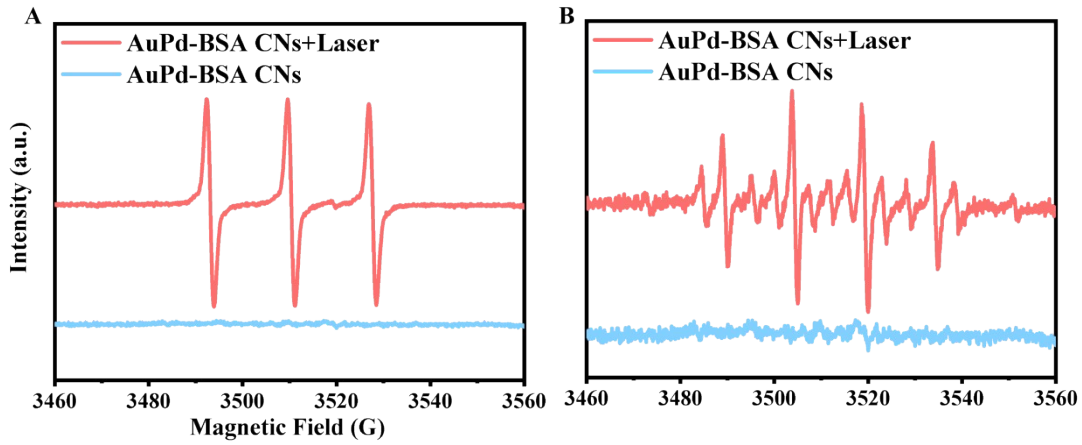

Figure S4. ESR analysis of A) $^1O_2$ and B) •OH production. (TEMP and DMPO were used as the spin-trapping agent, respectively.)

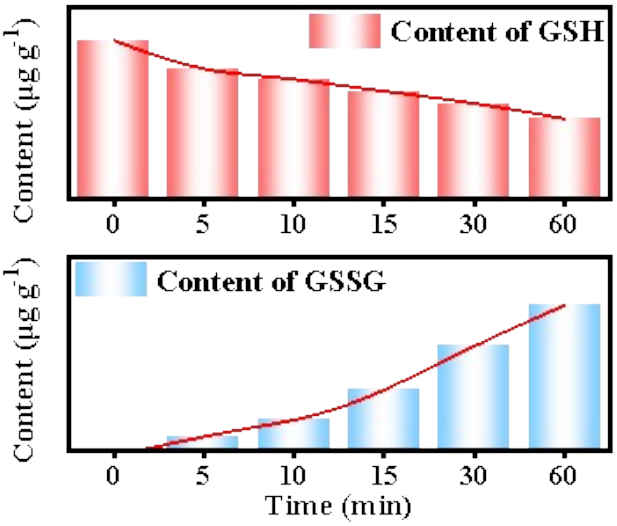

Figure S5. The changes in content of GSH and GSSG over time.

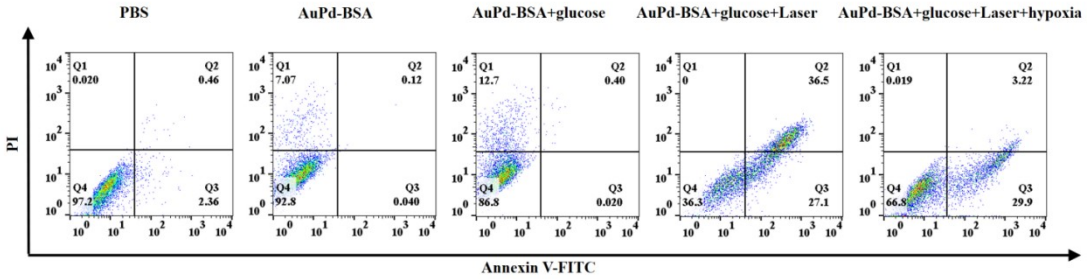

Figure S6. The flow cytometer analysis of annexin V-FITC/PI-stained cells after different treatments.

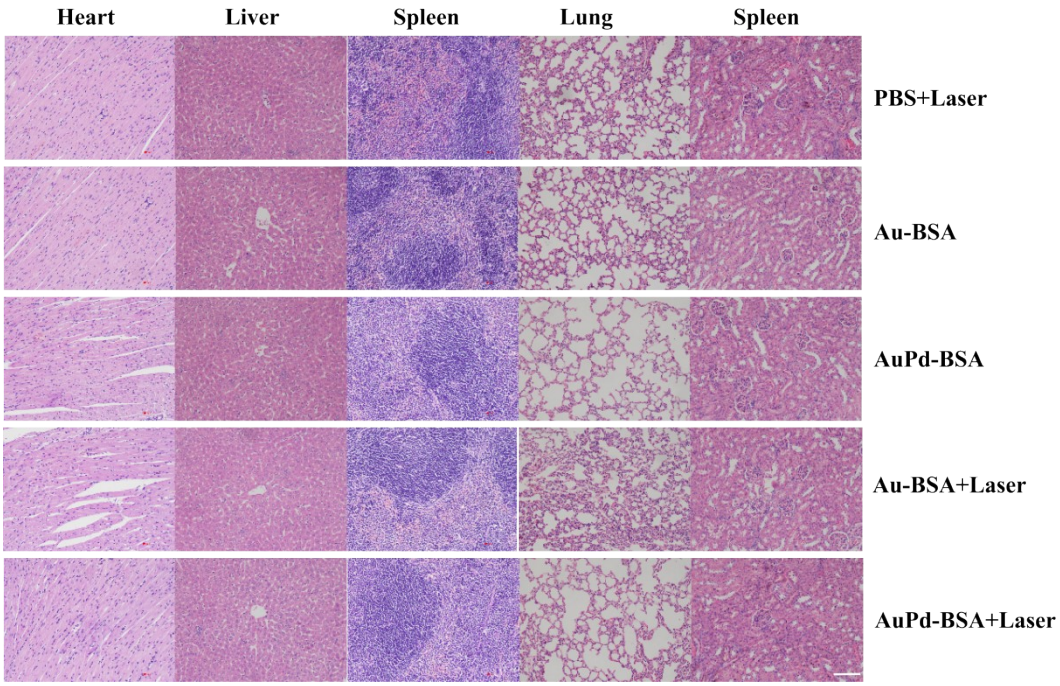

Figure S7. Histological H&E staining of major organ tissues in different groups. Scale bar: 200μm.

Table S1. The Michaelis-Menton constant (Km) and maximum reaction rate (Vmax) of as prepared AuPd-BSA and catalysts with H_2O_2 as the substrate.

Catalyst	Substrate	K_m(mM)	V_{max}(μM s^{-1})	References
AuPd-BSA	H_2O_2	77.84	3.53×10^{-2}	This Work
Fe_2O_3	H_2O_2	86.43	3.05×10^{-2}	25
Bi-Au NPs	H_2O_2	119	0.0725×10^{-2}	26
Pt	H_2O_2	84.07	2.2×10^{-6}	27
PtFe	H_2O_2	217.6	8.182×10^{-2}	28
Cu-N-C	H_2O_2	19.94	2.01×10^{-1}	29
Zn-CuO	H_2O_2	71	3.0×10^{-3}	30